The Influence of the Tower and Nacelle in Actuator Line Simulations of Floating Offshore Wind Turbines

D. Green [1,*] M. Zormpa [1] C.Vogel [1]

[1]Department of Engineering Science, University of Oxford, UK

*dylan.green@eng.ox.ac.uk

❶ Research Question

Floating offshore wind turbine platform motions generate unsteady wakes that affect downstream power production and fatigue loading. Accurate modelling of floating wind farms therefore requires improved understanding of platform-motion-induced wake dynamics. However, the aerodynamic influence of the tower and nacelle is often neglected in numerical simulations. This study aims to:

(i) Assess the influence of the tower and nacelle on wake dynamics under different platform motions.

(ii) Evaluate lower-fidelity meshless methods as an alternative to dynamic meshing.

❷ Methodology

- Numerical setup based on the NETTUNO wind tunnel campaign [1].
- Large-eddy simulation using WALE model for closure.
- Divergence-free synthetic eddy method used to reproduce inflow turbulence ($I \approx 2\%$) [2].
- Wall-modelled wind tunnel boundary layers to reproduce wind tunnel blockage.
- Actuator line model (ALM) used for turbine blade representation.
- Potential-flow velocity sampling used during blade-force evaluation [3].
- Prescribed sinusoidal platform motions characterised by dimensionless frequency $f_p^\star = f_p D/U_\infty$, amplitude A_p, and dimensionless time $\tau = f_p t \pmod 1$.
- Fields decomposed into mean, coherent, and incoherent components: $(\cdot) = \overline{(\cdot)} + \tilde{(\cdot)} + (\cdot)''$ and the coherent std defined $\tilde{\sigma}^2(\cdot) = \overline{\tilde{(\cdot)}^2}$
- Comparison of two tower+nacelle models against experimental, blade-resolved, and ALM results.

Immersed Boundary Method (IBM)

The immersed boundary method is implemented using a Brinkman penalisation approach. Solid motion is imposed through a body force added to the momentum equations,

$$\boldsymbol{f} = \chi_s \lambda (\boldsymbol{u} - \boldsymbol{u}_s),$$

where $\chi_s \in [0, 1]$ is a mask function defining the immersed solid region, $\boldsymbol{u}$ is the fluid velocity, $\boldsymbol{u}_s$ is the prescribed solid velocity, and λ is a penalisation factor. The value of λ is selected to enforce the solid motion accurately while avoiding excessive numerical stiffness.

Dynamic Mesh Method (DMM)

The dynamic motion is represented by deforming the computational mesh in response to prescribed structural motion. Mesh displacement is obtained solving

$$\nabla \cdot (\gamma \nabla \boldsymbol{d}) = 0,$$

where $\boldsymbol{d}$ is the mesh displacement vector and γ is a diffusivity defined as the inverse of the distance to the moving body, ensuring smooth deformation away from solid boundaries. The resulting displacement field is then used to update the mesh. Near-wall flow is modelled using a wall model.

❸ Cases

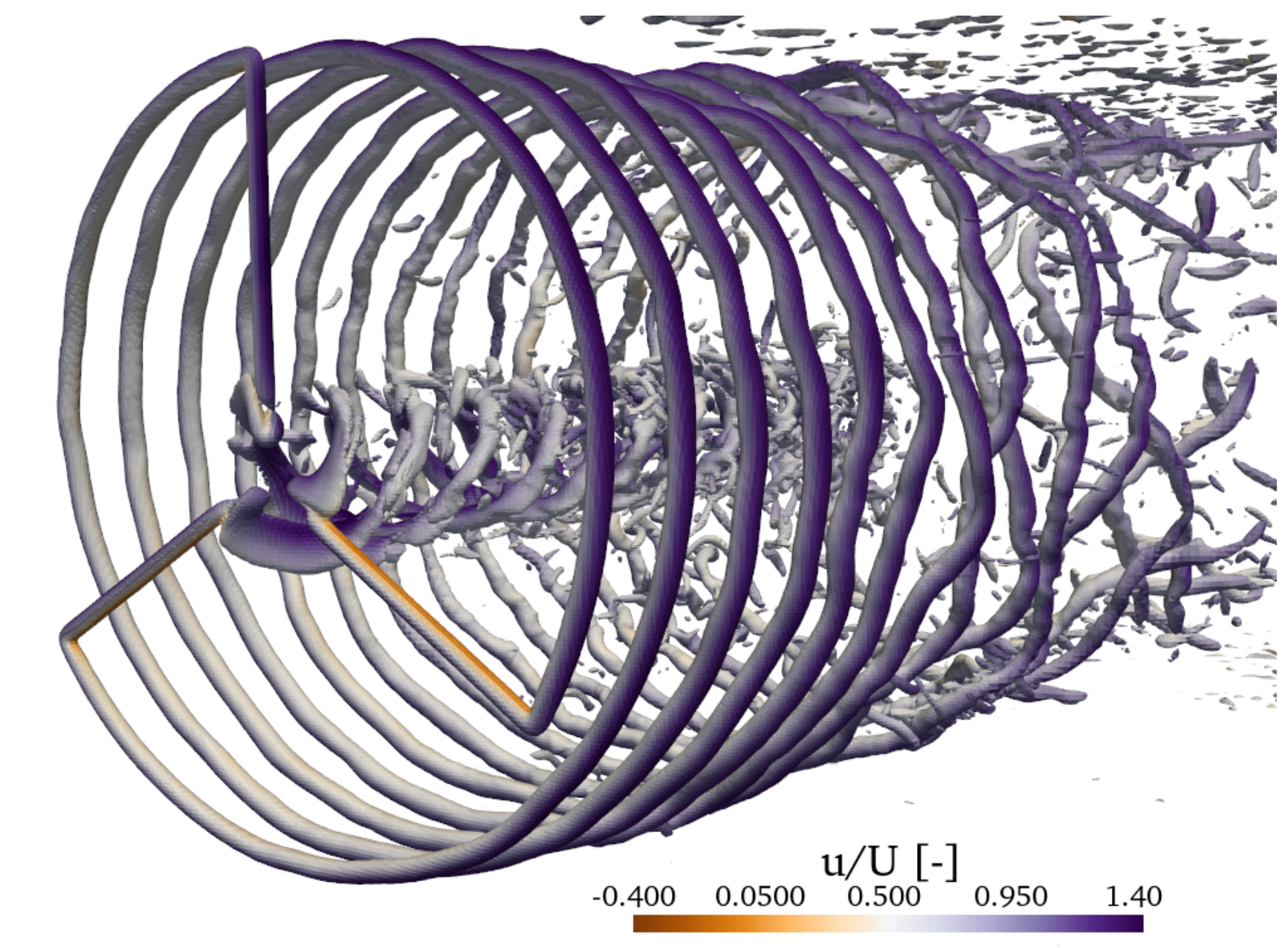

Case Keys

- **AL-XX:** ALM blades + no tower/nacelle
- **AL-IB:** ALM blades + IBM tower/nacelle
- **AL-DM:** ALM blades + DMM tower/nacelle
- **BR-DM:** Resolved blades + DMM tower/nacelle [4]
- **EXP:** Experimental data [1]

(a) AL-XX

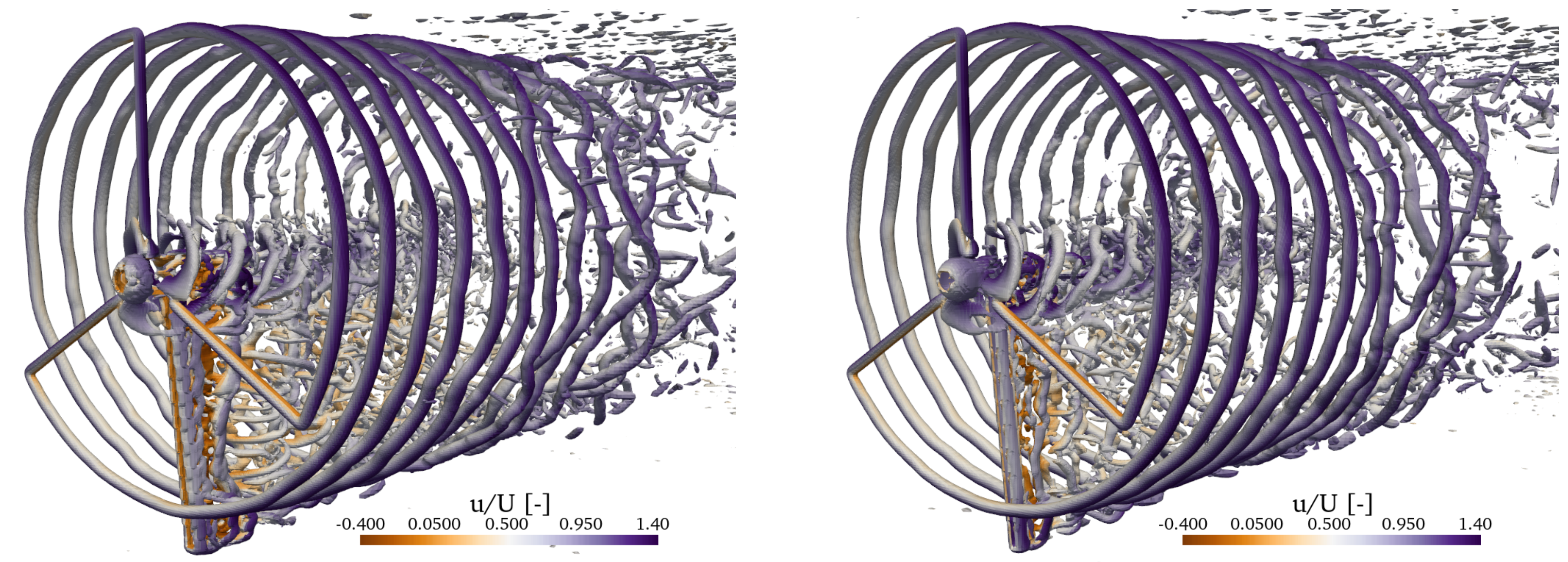

(b) AL-IB (c) AL-DM

Figure 1. Instantaneous snapshots of the wake showing Q-criterion contours coloured by the normalised streamwise velocity u_x/U_∞ for a rolling turbine with $(f_p^\star, A_p) = (0.30, 1.9°)$.

❹a Results: Load Response to Motion

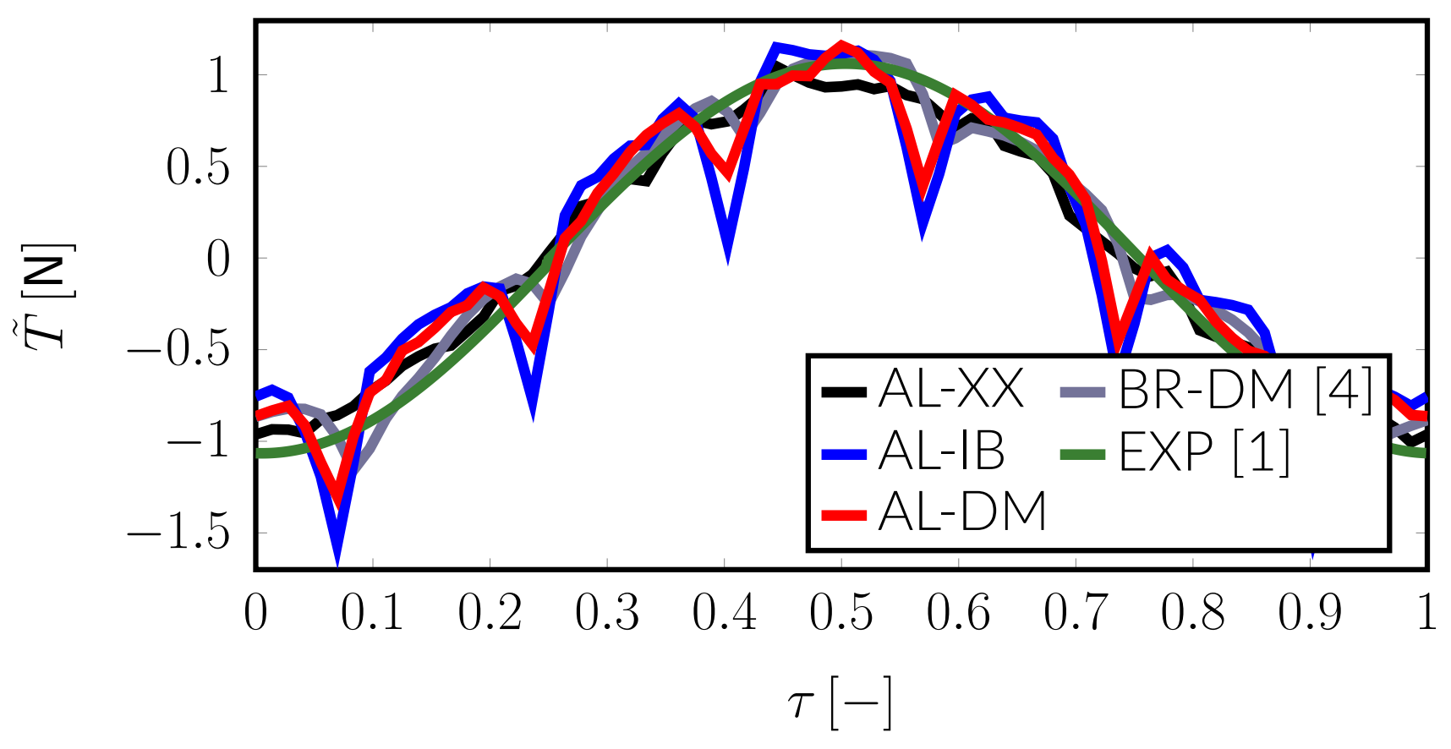

Figure 2. Coherent component of the rotor thrust under pitching motions characterised by $(f_p^\star, A_p) = (1.19, 0.3°)$.

	$\overline{T}$ [N]	$\Delta T^{f_p^\star}$ [N]	$\Delta T^{f_b^\star}$ [N]
AL-XX	35.71	0.955	0.027
AL-DM	35.76	0.965	0.207
AL-IB	35.66	0.949	0.325
BR-DM [4]	35.01	1.015	–
EXP [1]	36.19	0.957	–

Table 1. Time-averaged thrust, $\overline{T}$, and amplitudes of thrust oscillation at blade-passing, $\Delta T^{f_b^\star}$, and platform, $\Delta T^{f_b^\star}$, frequency for a pitching turbine with $(f_p^\star, A_p) = (1.19, 0.3°)$.

Strong agreement with reference data at $f_p^\star$ but significant overprediction at $f_b^\star$. (Note EXP is filtered above $f_b^\star$.)

❹b Results: Wake Spectra

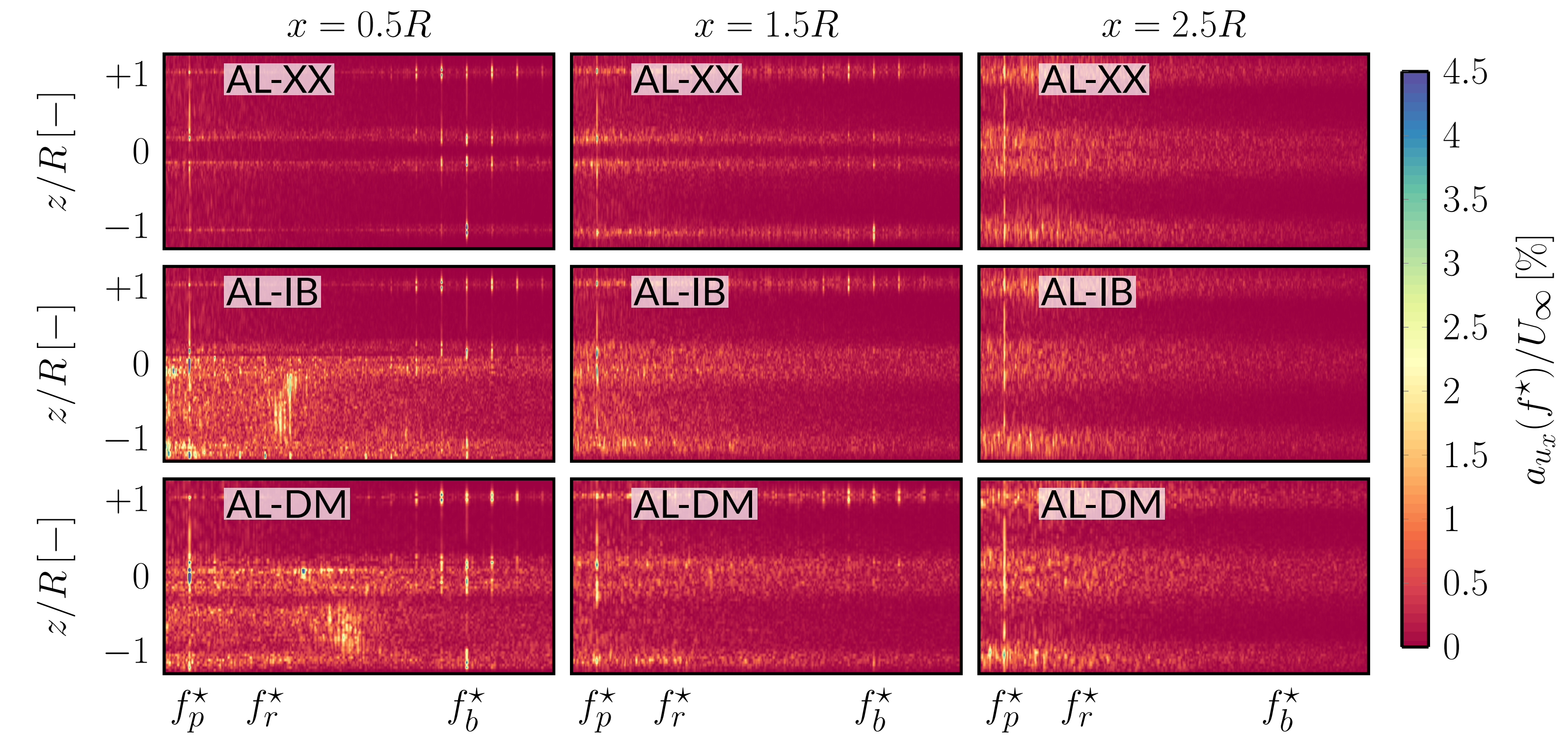

Figure 3. Wake streamwise velocity spectra as a function of the vertical distance, z, relative to the hub height at the initial rotor position for a pitching turbine with $(f_p^\star, A_p) = (0.60, 1.9°)$ at different downstream locations, $x = 0.5R, 1.5R, 2.5R$.

- Nacelle produces peak at $f_r^\star$ in very near wake.
- Tower shedding produced by both tower models albeit at a different frequencies.
- Asymmetric platform-induced velocity generates tones at $f_p^\star$, $f_b^\star$, $f_b^\star \pm f_p^\star$ and $f_b^\star \pm 2f_p^\star$.

❹c Results: Wake Dynamics

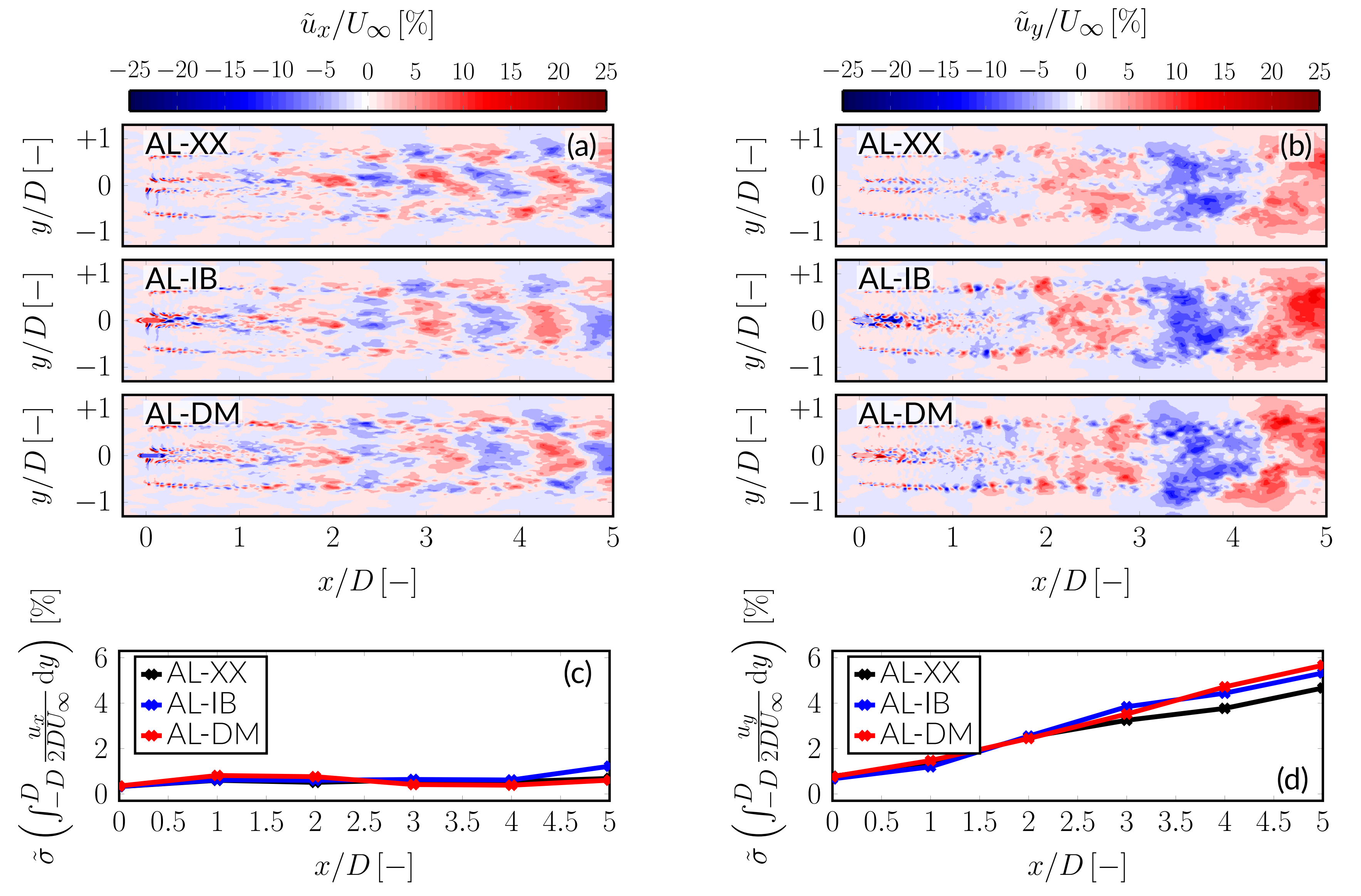

Figure 4. Coherent velocity contours at $\tau = 0.5$ and coherent standard deviation of the integrated velocity for (a,c) a pitching turbine and (b,d) a rolling turbine with $(f_p^\star, A_p) = (0.60, 1.9°)$ and $(0.30, 1.9°)$, respectively. The planes are located at the initial hub height. The velocity component is chosen to align with the platform induced velocity.

- Pitching motions appear to be largely unaffected by inclusion of tower+nacelle model.
- Roll induced meandering amplified by inclusion of tower+nacelle model.

❹d Results: Computational Expense

	AL-XX	AL-IB	AL-DM
Relative Cost	–	+7.5%	+ 365%

Table 2. Computational cost of each methodology relative to the AL-XX configuration.

AL-DM comes at significant cost relative to AL-XX and AL-IB.

Conclusions

1. Rotor thrust at $f_p^\star$ agrees well with validation data, while the response at $f_b^\star$ is overpredicted, likely due to amplification of tower-induced velocity deficit by the non-local sampling method.
2. Tower and nacelle effects introduce near-wake spectral content that is either diminished by $2.5R$ or advected out of the sampling plane by wake rotation.
3. Pitch-induced wake dynamics are largely insensitive to inclusion of the tower+nacelle model.
4. Inclusion of the tower+nacelle model amplifies roll-induced wake meandering.

Take Away Point:

⟹ Tower+nacelle effects depend strongly on the platform motion characteristics and may be important for accurate wake-response prediction.

Acknowledgment & References

The authors gratefully acknowledge Stefano Cioni and Alessandro Bianchini for providing data and further details regarding their CFD study [4]. This work used the ARCHER2 UK National Supercomputing Service through the EPSRC Access to HPC project, Wake Aerodynamics of Offshore Wind Turbines. The authors acknowledge support from DG's EPSRC studentship (no. EP/S023801/1) and CRV's UKRI Future Leaders Fellowship (no. MR/V02504X/1).

[1] A. Fontanella et al. In: *Wind Energy Science* 10.7 (2025), pp. 1369–1387.
[2] R. Poletto, T. Craft, and A. Revell. In: *Flow, Turbulence and Combustion* 91.3 (2013), pp. 519–539.
[3] Justine Schluntz and Richard H. J. Willden. In: *Wind Energy* 18.8 (2015), pp. 1469–1485.
[4] Stefano Cioni et al. In: *Ocean Engineering* 341 (2025), p. 122746.